2023

Expression of hTyr in Drosophila as a Novel Model of Parkinson's Disease

Madeleine Callan

Expression of hTyr in *Drosophila* as a Novel Model of Parkinson's Disease

A Thesis Presented

by

Madeleine J. Callan

To the Keck Science Department

of

Claremont McKenna, Scripps, and Pitzer Colleges

In Partial Fulfillment of

The Degree of Bachelor of Arts

Senior Thesis in Neuroscience

April 27, 2023

Abstract

Parkinson's disease is a debilitating and often deadly neurodegenerative disease affecting a growing and large population. Its etiology has long remained elusive, and because no other organisms have Parkinsonian-like diseases, it is difficult to study PD using model organisms. Neuromelanin (NM), an insoluble melanin synthesized in the dopaminergic synthesis pathway in DA neurons, has recently been implicated in PD as a major causal factor. At high levels in DA lysosomes, it functions as a proteostatic pathway inhibitor–blocking dopaminergic neurons from breaking down harmful molecules until the lysosomes eventually degenerate as well as triggering autophagy, inflammation, and total neurodegeneration. Recently, neuromelanin was first artificially expressed for the first time in a model organism by way of AAV-injection of hTyr into the rat substantia nigra pars-compacta (SNpc). We attempted to produce a PD model in *Drosophila melanogaster* by way of UAS expression of hTyr that is comparatively accurate, broadly useful in PD research and provides different advantages than a NM rat model. We created this first ever *Drosophila*-compatible pUAST-hTyr plasmid by cloning a pUAST plasmid and a hTyr mammalian plasmid. We used young and old WT Canton S flies to gauge a climbing assay and activity monitor assay for usefulness for testing WT and hTyr flies on negative geotaxis, spontaneous activity and circadian rhythm patterns. While at the completion of this project the hTyr flies are still being mated to complete the transgenic line and thus no data for those flies is available, we soon will have achieved the creation of the first-ever pUASt-hTyr flies for PD research and have provided a comprehensive and complete launching point for the next project involving the hTyr fly line.

Table of Contents

Introduction

The Impact and History of Parkinson's Disease:

An increasingly elderly world population is driving the need to cope with aging-related diseases. In the United States alone, life expectancy has risen almost 10 years on average in the last 50 years–and is expected to raise another 6 by 2060[1]. Humans continue to live longer and longer due to numerous public health revolutions. Increases in vaccination rates, anti-smoking marketing campaigns, and promotion of lifestyle changes such as exercise and healthy eating are just a few of the social revolutions that have prolonged human lifespan in the last 50 years[2,3]. While these revolutions have benefited humanity in many ways, age remains as the main risk factor underlying many common and deadly afflictions such as cardiovascular disease, cancer, and neurodegenerative diseases[4]. Newly common neurodegenerative diseases include Huntington's disease, amyotrophic lateral sclerosis, Alzheimer's disease, and more–the vast majority of which involve the progressive degradation of certain neuronal populations underlied by buildup of molecular blockages[5,6], and with them, the loss of quality of life and shortening of lifespan.

Parkinson's disease (PD) is no different. Its prevalence is increasing with time–the WHO claims that Parkinson's disease cases per million have doubled between 1994 and 2019 with 8.5 million total global cases recorded in 2019[7]. The symptoms include slowness of movement (bradykinesia), other motor deficits such as weakness and tremors, painful muscle stiffness, cognitive disorders, sleep disorders and more[7,8]. Many that develop Parkinson's disease also develop dementia and eventually die from complications from the disease.

Given its increasing prevalence, associated mortality and propensity to reduce the quality of life of those affected, Parkinson's disease research has steadily increased over time–but not without a messy research history obscuring many of the causal advances made in the field. Although Parkinson's disease was named in 1817, it was not until 1957 when Arvid Carlsson and his colleagues answered the question of how L-DOPA (L-DOPA delivers DOPA to the brain, which is a precursor molecule to dopamine) treated parkinsonian symptoms and found that dopamine was linked to Parkinson's disease[9,10,11,12]. Carlsson demonstrated that rabbits treated with reserpine, a drug that induces PD-like symptoms when administered, could rescue their motor deficits when treated with L-DOPA[9,10,11]. He also demonstrated that there were high dopamine (DA) levels in the rabbit striatum: the brain region known to control the elements of motion that were lost in the reserpine-treated rabbits[11]. Follow-up experiments from German and Japanese scientists found the DA ratios to be similar in the human striatum and also found high levels in the human substantia nigra pars compacta (SNpc) and ventral tegmental area (VTA)[9]. The DA in these areas was found to be deficient in those with Parkinson's disease. Later experiments found neurodegeneration of dopaminergic neurons projecting from the SNpc to the striatum in PD. The striatum–especially the dorsal striatum–is an area in the brain especially linked to movement control/initiation, which cemented the functional loss of dopaminergic signaling as the hallmark cause of Parkinson's disease symptoms[9,10].

Following Carlsson's experiment and the ones that followed up on it, two questions remained: could L-DOPA be used to treat PD in humans, and what causes the neurodegeneration of the dopaminergic neurons in the SNpc to cause the lack of

DA in the striatum? George Cotzias, a New York neuropharmacologist, answered both questions. He tested a new form of high-dosage L-DOPA administration as a treatment to PD in humans, and wanted to see if it had any effect on the neurodegeneration of dopaminergic neurons in the SNpc as well[9,10,13]. Cotzias believed that the neurodegeneration of the DA neurons in the SNpc was due to a lack of a compound called neuromelanin (NM) in those neurons–brought about by the recent finding that post-mortem PD patients' brains lacked NM in that area[14]. Therefore, his hypothesis was that high-dosage L-DOPA would rescue symptoms as they had in Carlsson's rabbit study and that it would rescue NM levels in the SNpc[9]. While he did not find anything new in the study regarding neuromelanin despite it being a motivator in his investigation, high-dosage L-DOPA proved to be remarkably effective as a treatment for the patients in the study–catapulting the field of Parkinson's disease research to a L-DOPA and dopamine-dominated phase[9,13]. Over time, it was understood that L-DOPA was an effective treatment because of its status as a direct precursor to dopamine–the aforementioned catecholamine that is deficient in PD patients, especially in the striatum. However, no one found evidence to prove that administration of L-DOPA treats any of the underlying factors causing PD and it only delays the progression of symptoms[9]–meaning that more work needed to be done to understand Parkinson's better.

Researchers focused on the dopamine synthesis pathway following Cotzias' landmark study, and particularly they focused on researching the synthesis of the aforementioned molecule neuromelanin. The papers published in the next decades suggested that neuromelanin is not a downstream product of the neuronal activity of the enzyme tyrosinase (TYR) as it is in melanocytes, but by tyrosine hydroxylase (TH)--the

rate-limiting enzyme in DA production (**Figure 1)**[9,15,16]. Initial studies did not find any corollary differences in TH (or TYR) and Parkinsons' disease–causing the field to move away from the two enzymes as actors of interest in PD etiology[9,17,18]. Neuromelanin was also pivoted away from as animal models of neuromelanin are non-existent–while NM does exist in some other mammalian species, it does not exist in nearly the same concentration as humans (where it is rich enough in certain brain areas to be observed macroscopically)[14,19]. The field moved on to studying other biochemical markers of Parkinson's disease such as tau tangles and alpha-synuclein. It would take decades for neuromelanin to be reconsidered as a possible player in the underlying pathology of Parkinson's disease, meaning that little direct research was done in the decades following Cotzias' L-DOPA revolution.

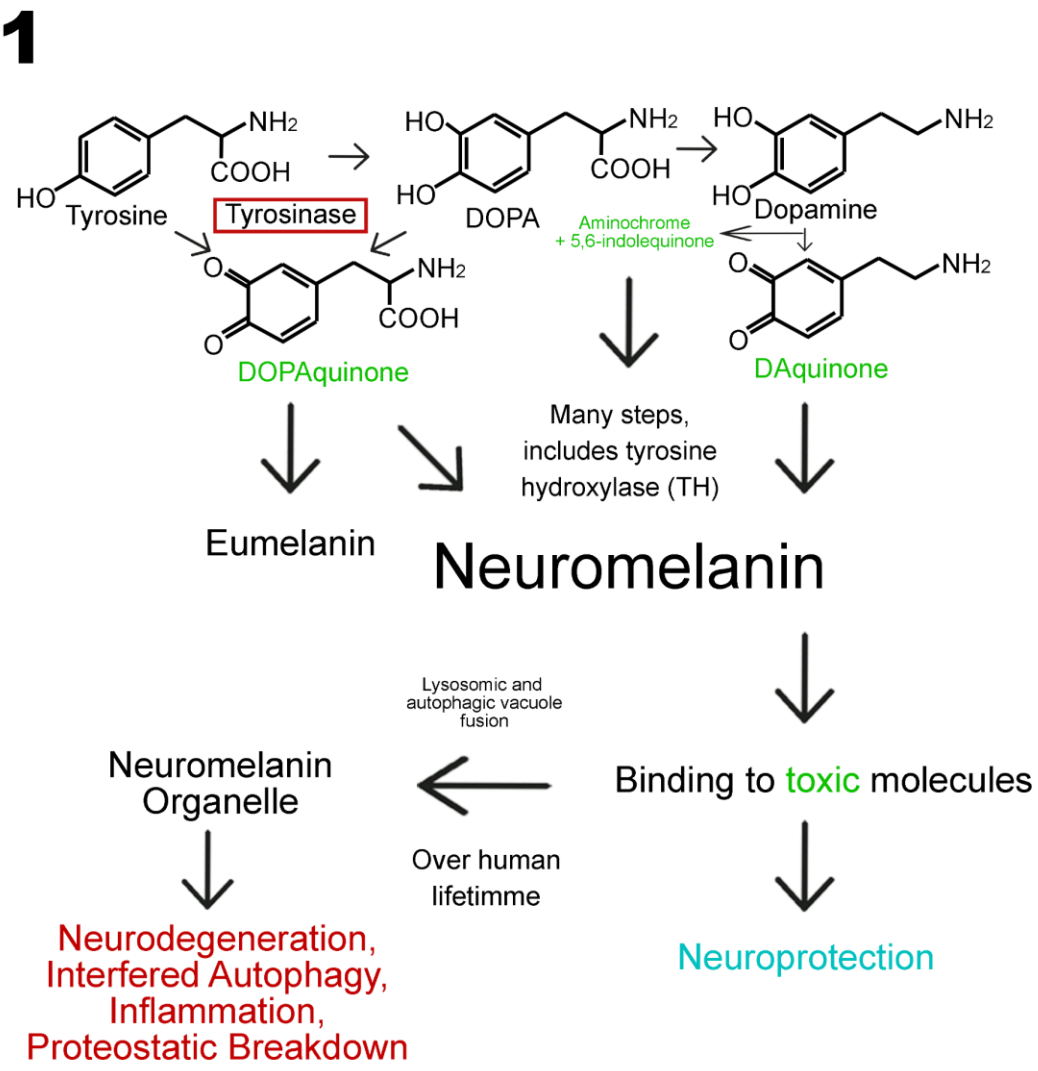

Figure 1: The dopaminergic influence on the synthesis of neuromelanin by tyrosinase and other enzymes and its overall effects on cell function post-synthesis.

Shows the relevant molecules and enzymes involved in neuromelanin production as well as its etiology in the dopaminergic cell at different points in time. The synthesis of neuromelanin includes tyrosinase (hTy)r as seen in the top left section, and involves the elimination of toxic molecules (shown in green) through its synthesization[15,20,21,22,46]. Neuromelanin itself also binds to many toxic molecules including dopaminergic intermediaries and ROSs, which leads to neuroprotection at low amounts. However, over time, the insoluble neuromelanin is collected by the cell into autophagic vesicles and fused with lysosomes, which creates unsustainable amounts of damaging neuromelanin

organelles in certain individuals[15,21,23,,24,28,48]. This figure is modified from Mousavi, S. et al. 2018[46] and Sulzer, D. et al. 2018[48].

Neuromelanin: A Causal Factor of SNpc Dopaminergic Neurodegeneration in PD

Neuromelanin, a bon-a-fide melanin compound that only exists in the brain[20,21], was seriously considered as a part of Parkinson's disease pathology due to its depletion in Parkinson's disease brains–especially in the SNpc, an area rich with dopaminergic neurons that innervates the striatum[14]. As discussed, the enzymes tyrosinase (TYR) and tyrosine hydroxylase (TH) are involved in the conversion of tyrosine to DOPAquinone, which is modified several times before it is eventually converted into neuromelanin (**Figure 1**)[15,20,21,22,46]. Evidence suggests that neuromelanin exists in dopaminergic cells as a way to quickly rid the cells of toxic dopaminergic intermediaries such as DOPAquinone and a shielding molecule that can protect cellular systems against redox active metals and toxins through binding **(Figure 1)**[22,46]. However, neuromelanin is insoluble,which eventually causes NM buildup in autophagic vacuoles **(Figure 1)**[23,48]. These merge with lysosomes in an attempt to break the NM down, but due to its insolubility, it builds up and attracts lipids and toxic dopaminergic byproducts to eventually form neuromelanin organelles (**Figure 1**)[23,48]. It is also known that NM starts building up in the brain at three years old and steadily continues over a human lifetime[21,24]. Taken together, Parkinson's researchers speculated that neuromelanin's co-opting of lysosomes over a long period of time may have the effect of bogging down the cell's system for degrading unwanted molecules–clogging the cell with toxins which lead to interference with autophagy and eventually full proteostatic failure (**Figure 1**)[15,21,23,25,48]. Studies have shown that higher neuromelanin increases alpha-synuclein

levels in SN neurons. In turn, alpha-synuclein induces the compensatory expression of neuromelanin by increasing the amount of cytosolic DA[26,27]. Alpha-synuclein is a known protein implicated in Parkinson's disease etiology. These findings and more, which slowly came out over the course of the 21st century, began to refocus some of the field's attention back on neuromelanin as a major part of PD etiology as well as the enzymes involved in its production.

Carballo-Carbajal's groundbreaking 2019 study culminated what had been found after the turn of the century into the first ever neuromelanin-based Parkinson's disease animal model in rats[15]. Model organism development is particularly important in Parkinson's disease research due to there being no natural occurrences of the phenomenon or any comparable analogues outside of humans[21]. This may be due to neuromelanin only existing in high quantities in humans, which Carballo-Carbajal's findings support. Carballo-Carbajal expressed high quantities of neuromelanin in the SNpc in order to test the propensity for the addition of neuromelanin to induce PD-like symptoms. To do this, Carballo-Carbajal tested a new theory that has only taken hold in PD research recently: that tyrosinase exists in neurons and has sufficient activity in said neurons to contribute to neuromelanin production[15,28-30]. Seeing as the version of tyrosinase seen as humans is distinct, Carballo-Carbajal chose human tyrosinase (hTyr) to overexpress in rats via direct injection through adeno-associated virus (AAV)--a viral transmission system that can deliver a gene directly into infected cells. Post injection mice showed drastically increased neuromelanin production in the SNpc. Rats 2-4 weeks post-injection showed hTyr expression in 80-90% of their SNpc neurons and by 2 months the SNpc could be imaged macroscopically by its NM expression. This on its

own was remarkable, as this experiment provided evidence that hTyr introduction into a mammalian brain is sufficient for dopaminergic SNpc cells to produce NM. Follow-up experiments showed extremely similar etiology to human PD in these rats, in neurodegeneration, dopaminergic dysfunction, proteostatic failure, inclusions and symptoms, including bradykinesia. In addition, NM accumulation did not stop over time, and the progression of the etiology mimicked human PD progression on an adjusted timescale. Alpha-synuclein was also found to be dispensable for NM-induced PD-like inclusions and neurodegeneration, which supports neuromelanin as an instigating causal factor in PD etiology. Critically, Carballo-Carbajal also found that inducing lysosomal exocytosis, the process by which lysosomes are fused to the cell's outer membranes and the lysosome's contents are dumped into the extracellular space, could stop NM-induced degeneration and halt or even reverse progression of PD symptoms. This is a revolutionary finding and necessitates further research.

The Case for and Process of Making the Drosophila Neuromelanin Model

While Carballo-Carbajal created the first-ever neuromelanin model of PD in rats, we believe that there exists a strong need for a similar model in a more tractable model organism. *Drosophila melanogaster*, a class of insects commonly known as the fruit fly, are ideal model organisms for quick turnaround and/or highly exploratory studies due to their cheap cost, easy upkeep, powerful molecular binding, robust and accessible genetic tools, invertebrate status and short lifespan[31]. The existence of public, 3D connectomes for the fly brain make *Drosophila* ideal for studies that seek to explore phenomena at the systems or structural level[32], and the relative ease at which the brain

can be accessed is a major asset for wide-scale brain imaging and dissection. *Drosophila* is an established model organism in neurodegenerative disease research, meaning there are multiple established assays for testing different elements of PD-related phenotypes–from reduced negative geotaxis/bradykinesia (climbing assays)[33,34] to spontaneous activity/circadian rhythm abnormalities (activity monitor assays)[35-37]. The creation of the model organism itself is also critically informative–if the expression of hTyr in dopaminergic neurons in flies does not lead to PD-like etiology, we would gain information about what conditions are necessary *in vivo* to facilitate NM expression and/or PD-like etiology.

Additionally, revolutionary and recent experiments like Carballo-Carbajal's experiment must be recreated in different model organisms not only for validity but to test out whether their revolutionary lysosomal exocytosis findings are valid and can be extended to the development of novel treatments[15]. In the example of lysosomal reversal of NM-laden dopaminergic degeneration; if this can be recreated in other model organisms, it will be extremely revolutionary in the field of Parkinson's disease as it would show that this finding is not only more robust, but generalizable to any NM-laden dopaminergic neurons, which increases the research potential of promoting exocytosis in humans. *Drosophila*'s relatively low turnover time and low cost in terms of treatment testing would make it the ideal organism to test whether exploring lysosomal exocytosis is a fruitful PD treatment pursuit and to test the validity and efficacy of similar findings.

For these reasons and more, the goal of this thesis was to create a neuromelanin Parkinson's disease model in *Drosophila* by expressing hTyr in dopaminergic neurons to test whether hTyr expression is a valid method of inducing NM-production in

Drosophila and, if so, to test whether this production creates flies with PD-like symptoms. We created the first ever hTyr fly line by first cloning a hTyr/3xFLAG sequence from an existing mammalian plasmid into a *Drosophila* backbone **(Figure 2)**. While this cloned plasmid was injected into fly larvae, we collected data on flies separated by 3 weeks of age to set a baseline for the negative geotaxis, spontaneous activity and circadian rhythm assays with the older flies serving as a proxy for the hTyr flies. Additionally, we performed dissections on each driver line we wished to mate with our hTyr line to prove that each driver line is expressed in the appropriate neurons and to collect comparison images. Currently, we are working to establish homozygous stocks of hTyr flies to gauge its potential as a PD model.

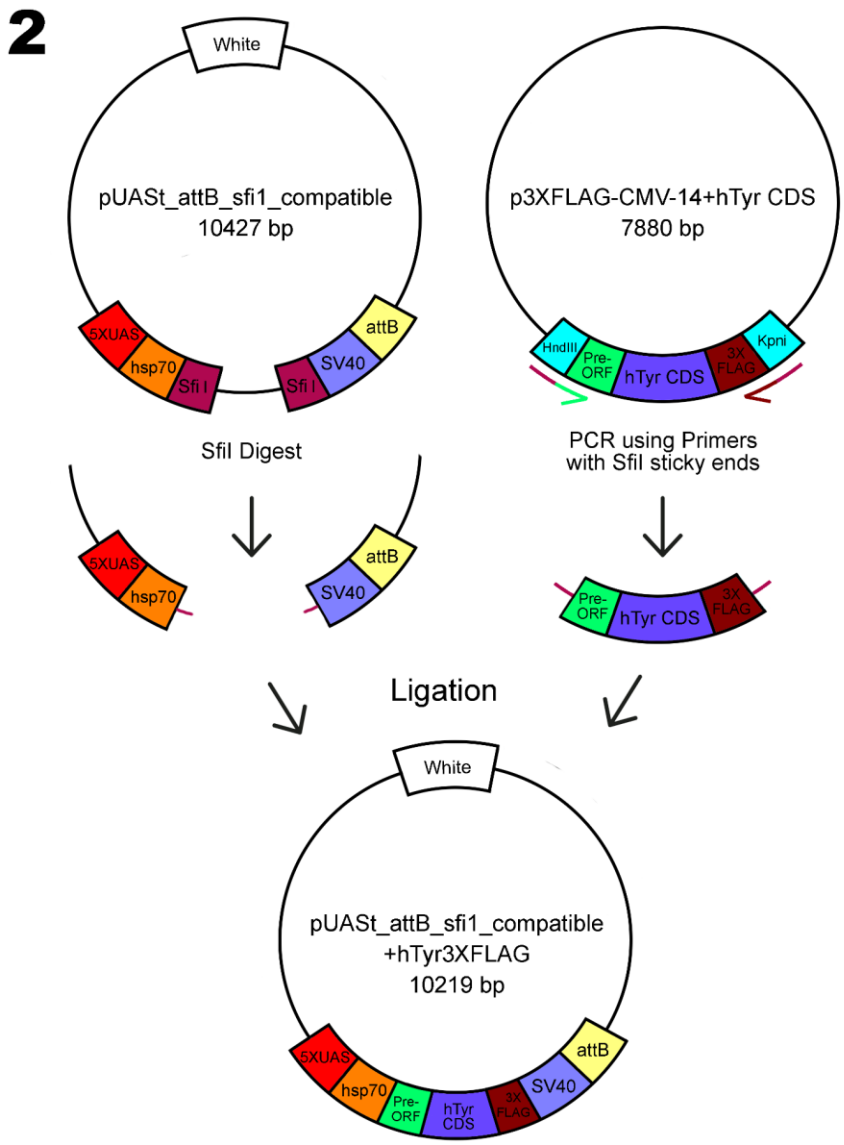

Figure 2: Simplified cloning process used to create the pUAST_attB_sfI compatible+hTyr3XFLAG plasmid from *Drosophila* pUAST_attB_sfi1_compatible plasmid and p3XFLAG-CMV-14+hTyr CDS plasmids. pUAST_attB_sfiI_compatible was provided by the Groth lab[45]. p3XFLAG-CMV-14+hTyr CDS was ordered off of addgene and was created by the Halaban lab[41]. After these plasmids were extracted by miniprep from the bacterial colonies they were stored in, an SfiI digest was performed to cleave the pUASt plasmid at its SfiI cut sites leaving sticky ends (shown in maroon). Primers hTYR_SfiI_F and hTYR_SfiI_R (full sequences in supplementary information) were used to perform PCR on the hTyr mammalian backbone plasmid to create the fragment with sticky ends as shown. The two DNA strands were ligated as shown to create the combined plasmid.

Materials & Methods

Cloning pUASt-hTyr plasmid in Drosophila

hTyr-CDS from a mammalian plasmid was cloned into a pUAST plasmid using standard cloning procedures. More information on the procedures used and methods used to verify them can be found in the supplemental information. Transgenes were introduced into flies using an established transgenesis system (phiC31 integrase[55], Rainbow Transgenic Flies Incorporated, Camarillo CA).

Drosophila Driver Line Genetics for Tissue-Specific Expression

ELAV-GAL4 mated with a GOI (gene of interest)-UAS line (ELAV-GAL4/UAS-GOI) would express the GOI in all neuronal tissue **(Figure 3)**. NPF-GAL4/GOI-UAS expresses GOI in all NPF-producing neurons **(Figure 3)**. ple-GAL4/GOI-UAS expresses GOI in all dopaminergic neurons **(Figure 3)**. WT controls are also used. All driver lines as well as all WT flies were ordered from the Bloomington Drosophila Stock Center (NIH P40OD018537).

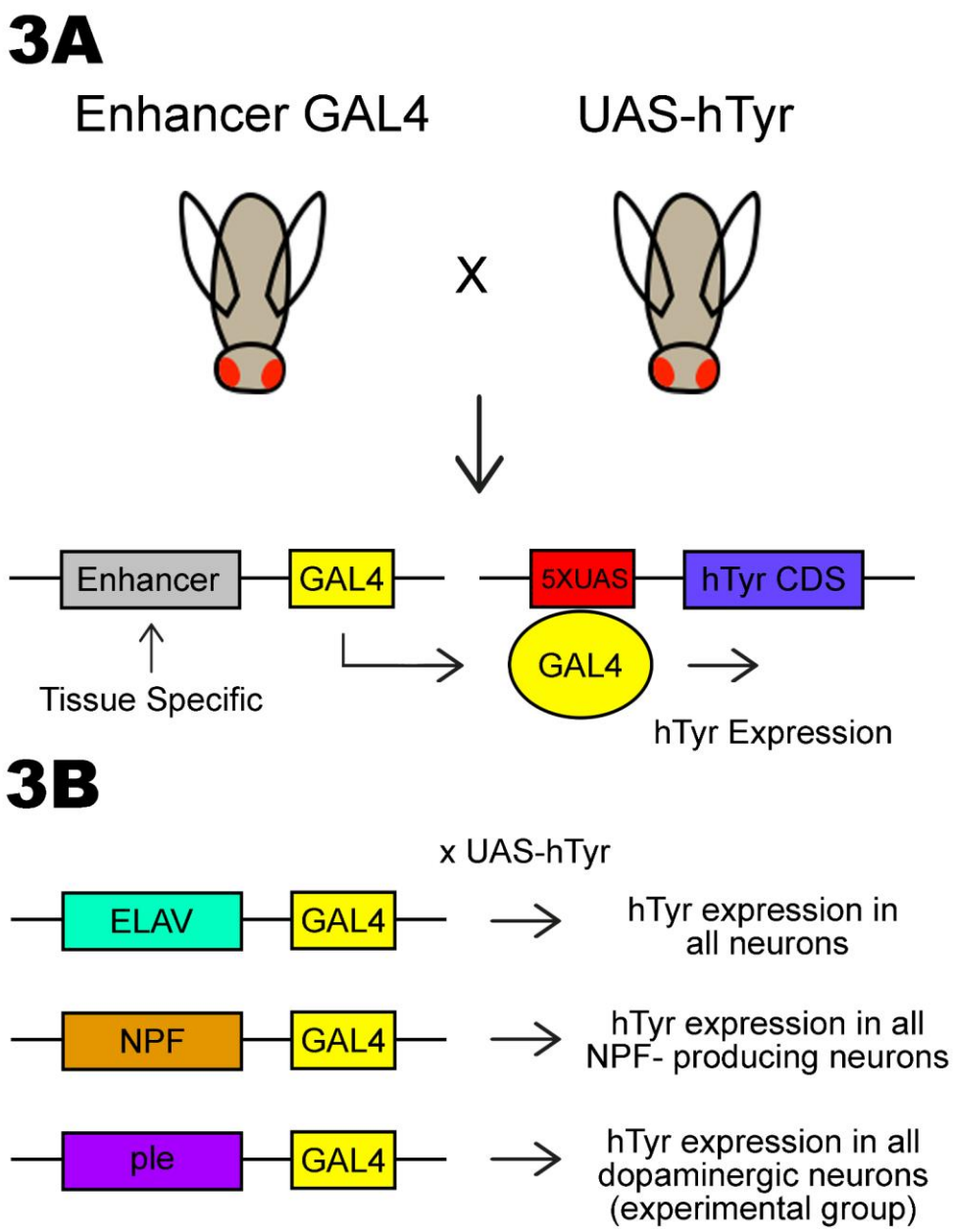

Figure 3: GAL4-UAS binary expression system allows for differential tissue-specific expression of hTyr.

A. Shows the mechanism by which the GAL4-UAS expression system allows for hTyr to be expressed based on the identity of the enhancer sequence. B. Shows the driver lines that will be crossed with homozygous UAS-hTyr flies to produce tissue-specific hTyr expression. ELAV-GAL4 was selected as a control line to test the hypothesis that hTyr expression in all neurons will produce the same results as only expressing it in dopaminergic neurons, as well as a control to make sure that there are no unrelated issues with global neuronal expression. NPF-GAL4 was selected as a functionally and in some areas locationally-similar control to DA neurons. ple-GAL4 allows for only dopaminergic

expression and would be our main experimental group. A fourth control driver line that does not cause any substantial hTyr expression is not shown (**Figure 4**).

Drosophila Culture

Control flies were housed in groups of 20 in vials, separated by sex and genotype, with 2 mL of standard agar-cornmeal-yeast-sugar media (10 g/L agar, 30 g/L yeast, 19 g/L sucrose, 38 g/L dextrose, 91 g/L cornmeal, 11 mL/L acid mix (41.8% propionic acid and 3.5% phosphoric acid), and 15 mL/L 10% methylparaben) in humidified incubators at 25 °C on a 12:12 hour light/dark cycle). The control flies were transferred to fresh vials every 3-4 days.

Drosophila Brain Dissection and Imaging

Brains were dissected and imaged in 1xPBS. The images seen in this paper are overlays of images taken using a GFP filter and images taken using a white light on a microscope. ImageJ[52] was used to create images that have the white light as gray channel and the GFP image as green channel. White light images were taken at 0 gain and 200-300 ms exposure time, and GFP images were taken at 1.4 gain and 6-8 s exposure time.

Climbing Assay

~20 flies were transferred from food vials into testing vials and left to acclimate vertically for 1 hour with the food vials on top. After 1 hour, the food vials were removed from the testing tube with a stopper replacing them. The bottom of the tube was then sharply tapped on a hard, flat surface 5 times to collect the flies at the bottom and

startle them, which induces them to climb upwards. After 20 seconds of climbing, a photo is taken. The vial is divided into 3 equal portions of 10 cm which each have different scoring (3 for each fly in the top third, 2 for each fly in the middle, 1 for each fly in the bottom). The score is added together for each vial in each replicate, and each vial is testeed 3 times with at least 10 minutes between replicate. The average score across all 3 is then used for a t-test.

Spontaneous Activity and Circadian Rhythm Assay (DAM)

~20 flies were collected into 8 vials per replicate. They stayed in a tube with food and those tubes were then placed into an apparatus with a central sensor light that adds one to a tracker when a fly passes through it (peripheral sensor light data was collected but was too unreliable to use for this study). These 8 vials are placed into a light-proof container with a white light that comes on at 8:00 and turns off at 20:00 each day giving a day-night cycle of 12 hours each. The data was trimmed to only contain full 24 hour cycles. The integral was taken and compared across groups using a t-test for the spontaneous activity data. The raw data is graphed against a timeline to show activity across the day and periodograms were created using a Fourier analysis with Fisher's significance analysis to show patterns of rhythmicity.

Statistical Analyses

Two-tailed unpaired t-tests were conducted for analysis of climbing assay and spontaneous activity assay data with an alpha value of .05 in SPSS version 28.0.1.0. A standard Fourier analysis with Fisher's procedure significance test with an alpha value

of .05 was conducted for analysis of circadian rhythm periodicity (python code in the supplemental figure)[53,54]. In the figures, * represents .05 > p > .02, ** represents .02 > p > .01 and *** represents p < .01 **(Figures 5B, 6B, and 8)**.

Results

Cloning

As there is no existing record of any lab expressing human tyrosinase (hTyr) in *Drosophila,* we needed to create our own fly line that would express this protein. Because there has not been an hTyr fly line, there were also no readily available plasmids containing the hTyr coding sequence and *Drosophila*-compatible background. Therefore, we needed to clone the CDS from a different plasmid into a backbone compatible with *Drosophila.* The hTyr CDS along with a 3x FLAG tag was acquired from the Halaban lab (Addgene plasmid #32780)[41] (**Figure 2**), and we cloned it into the pUASt_attB_sfI compatible plasmid (**Figure 2**)[45]. Using ApE[51], we created a virtual clone of how the plasmid we would inject into flies would look (**Figure 2**). The cloning process is simplified in figure 2 and the primers and validation gels used to complete the cloning process are in the supplementary section.

Driver Lines to Verify Expression and Predict NM Granule Locations

hTyr was expressed in the flies using the UAS-GAL4 binary expression system[38] (**Figure 3**). UAS-hTyr flies were created as previously described (**Figures 1 and 2**). We chose to order a variety of GAL4 lines for our experimental hTyr flies to be crossed with as various control groups (**Figure 3**). ple-GAL4 crosses will express hTyr solely in

dopaminergic neurons, which we hypothesize will be sufficient to synthesize neuromelanin in *Drosophila* as it is in rats[15]. ELAV-GAL4 crosses would express hTyr in all neuronal populations. This would serve two functions. It would serve as a control to avoid possible confounding hTyr expression in non-neuronal tissues, but given that neuromelanin should only be expressible in dopaminergic neurons anyways, ELAV flies should also express neuromelanin and be viable models of PD. If the ple flies end up not expressing NM in key neurons, we would be able to use the ELAV flies to determine which neurons need to be affected in order to produce PD-like etiology. NPF-GAL4 crosses would express hTyr only in neurons that create neuropeptide F, a neuropeptide-Y-like neuropeptide that regulates some similar functions to dopamine in flies (sleep/wake cycle, motivation)[39]. As previously discussed, neuromelanin is a direct derivative from metabolites involved in the dopamine synthesis pathway, and necessitates other enzymes that are present in the dopamine synthesis pathway in order to be synthesized[20], and thus NPF neurons are a functionally (and locationally)-similar but structurally-divergent control. There would be WT control flies as well. All of these lines were mated with GAL4-GFP to create x-GAL4/UAS-GFP lines for verification.

All fly lines (**Figure 3**) as well as the unmated controls mated to express GFP were dissected and imaged (**Figure 4**). These dissections were done for the purposes of collecting images of non-hTyr brains to compare to future dissected hTyr brains and for verification that the drivers were expressing the GOI (gene of interest) in the correct brain locations. The images in figure 4 clearly show GFP expression in the appropriate brain areas for each line. ple-GAL4/UAS-GFP flies clearly showed GFP expression at

the dopamine PAM and PAL clusters from the anterior view, and expression in the dopamine PPL1, PPM1/2, PPM3 and PPL2 clusters from the posterior view (**Figure 4A**). NPF flies showed expected expression at the DM (**Figure 4B**). ELAV-GAL4/UAS-GFP flies showed global GFP expression with high expected expression in the eye tissue. WT control flies showed no detectable GFP expression. High brightness areas in the WT image are from residual tissues that show high brightness in all light.

We would compare these images to dissected x-GAL4/UAS-hTyr brains at different times in the fly life cycle to determine whether and where neuromelanin can be observed macroscopically, as well as any other brain abnormalities that may occur as an unexpected result of hTyr expression. Specifically, we would expect macroscopically visible dark NM granules in young ELAV-GAL4/UAS-hTyr and ple-GAL4/UAS-hTyr flies, and the brains of these two lines should look the same. It is plausible that the NM granules previously visible in young flies of these two lines would not be visible in older flies as neurodegeneration of DA neurons leads to NM spilling out into the extracellular space, reducing the concentrated, visible NM granules[15]. We would expect no visible NM in NPF-GAL4/UAS-hTyr flies or WT flies.

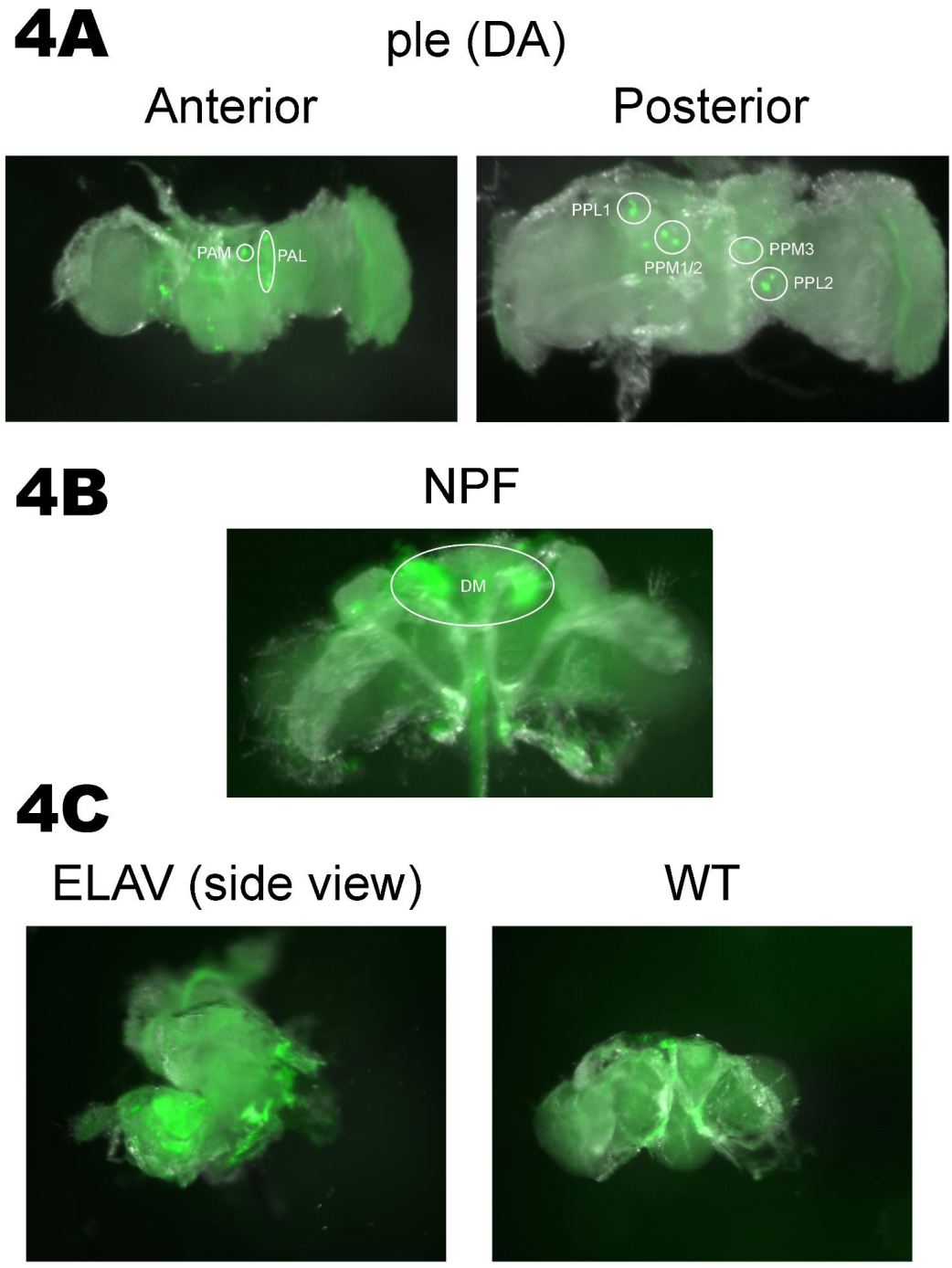

Figure 4: Dissected driver-GFP lines show appropriate GFP expression.

All images are combined GFP light/white light images with GFP in green. A: Two different brains from ple-GFP flies are shown. Both brains show brightness in the appropriate dopaminergic clusters. B: One brain from a NPF-GFP fly

is shown with appropriate brightness in the DM NPF cluster. C: ELAV-GFP and WT brains are shown with appropriate levels of global brightness (high and low, respectively).

Verification of Climbing as Quantification of Bradykinesia

As Parkinson's Disease is known to have robust negative effects on movement, and as rats in Carballo-Carbajal showed significant movement deficits due to developed bradykinesia[15], we employed a climbing-based negative geotaxis assay to determine the movement capabilities of our flies (**Figure 5A**)[33,34]. In addition, as neuromelanin builds up over time and as movement deficits typically worsen over the course of Parkinson's disease, we wished to see whether there were age-dependent effects on negative geotaxis[15,21,24]. As a baseline control for the hTyr flies and to quantify aging's typical effects on movement in flies we tested control flies eclosed 3 weeks apart (**Figure 5B**). Older flies have marked negative geotaxis deficits as compared to younger flies, and thus older flies thus serve as a hTyr proxy while the comparison between younger and older validates the assay as compared to established climbing assay data[21,24]. Both males and females showed a significant age-related difference where the 3 week older flies had significantly reduced movement in the assay (unpaired two-tailed t-test, n = 5 of 3 technical replicates, ~20 flies per experimental replicate, $t(8) = -11.276$, $p < 0.001$ (female), $t(8) = -20.909$, $p < 0.001$ (male)). As the hTyr homozygous line is still being developed, we do not currently have negative geotaxis data to compare against that shown in figure 5B, but if we observe hTyr flies to have significantly lower scores than their corresponding age group this will support hTyr flies as an accurate model of bradykinesia in Parkinson's disease[42].

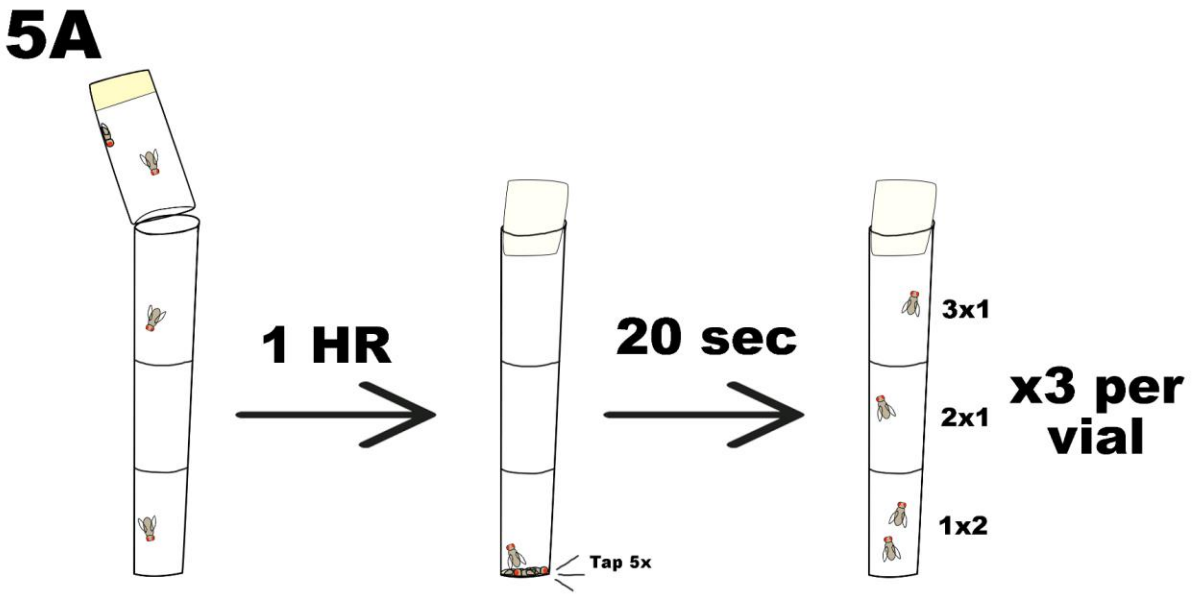

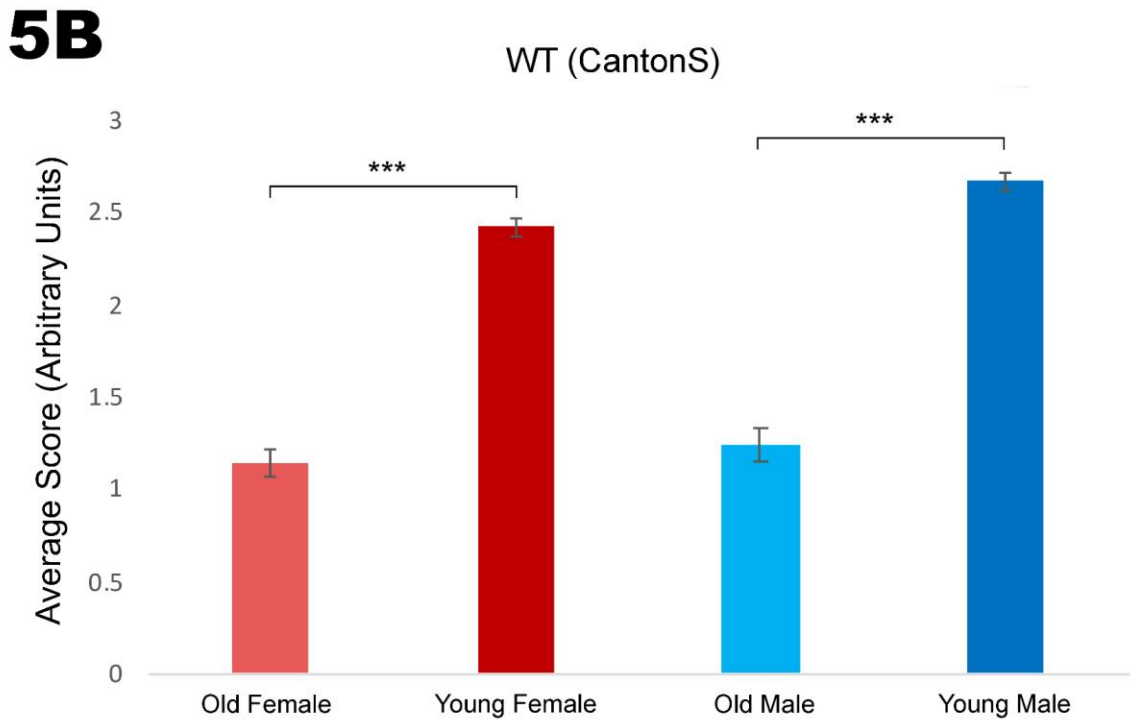

Figure 5: Older WT CantonS flies show significantly lower negative geotaxis scores than young flies (eclosed 3 weeks apart, young flies ~2 weeks old).

Climbing ability was used to assay negative geotaxis or general movement ability in flies. A. Climbing ability was measured by the fly's vertical distance traveled in 20 seconds after a disturbance. An example is shown with 4 flies in each tube but around 20 were used in each vial in the experiment. B. 89 old female, 98 young female, 85 old male, and 98 young male flies were tested in total. A significant decrease in climbing ability is seen in WT CantonS older

flies (n = 5 of 3 technical replicates, ~20 flies per experimental replicate, t(8) = -11.276, $p < 0.001$ (female), t(8) = -20.909, $p < 0.001$ (male)).

Verification of DAM as Quantification of Spontaneous Activity

One facet of the motor defects seen in Parkinson's disease is a low ability to initiate movement[21]. In flies, this can be represented by spontaneous activity measured using a single-beam *Drosophila* activity monitor (DAM) (**Figure 6A**)[37]. As a baseline control for the hTyr flies and to quantify aging's typical effects on movement in flies we tested control flies eclosed 3 weeks apart (**Figure 6B**). We expected to see a significant decrease in spontaneous activity from all younger flies to their sex-matched older flies, and as in the climbing assay, the older flies served as a rough proxy to the hTyr flies. We did see a significant decrease in the older female flies as opposed to female flies (unpaired two-tailed t-test, n = 2, ~40 flies per replicate, t(2) = -7.087, $p = .029$), but the male flies showed no significant difference (unpaired two-tailed t-test, n = 2, ~40 flies per replicate, t(2) = 1.344, $p = ns$). This is likely due to one tube in the old male dataset significantly skewing the data–however because of technical limitations (degrees of freedom could not go lower) this tube could not be removed from the data set. Therefore, adding more samples to the experiment would help determine whether this effect could be robustly seen in males as well. Regardless, in female hTyr flies, we would expect to see significantly less spontaneous activity as compared to WT CantonS flies in both age groups as well as a significantly larger difference between the two age groups than in WT flies[21,37].

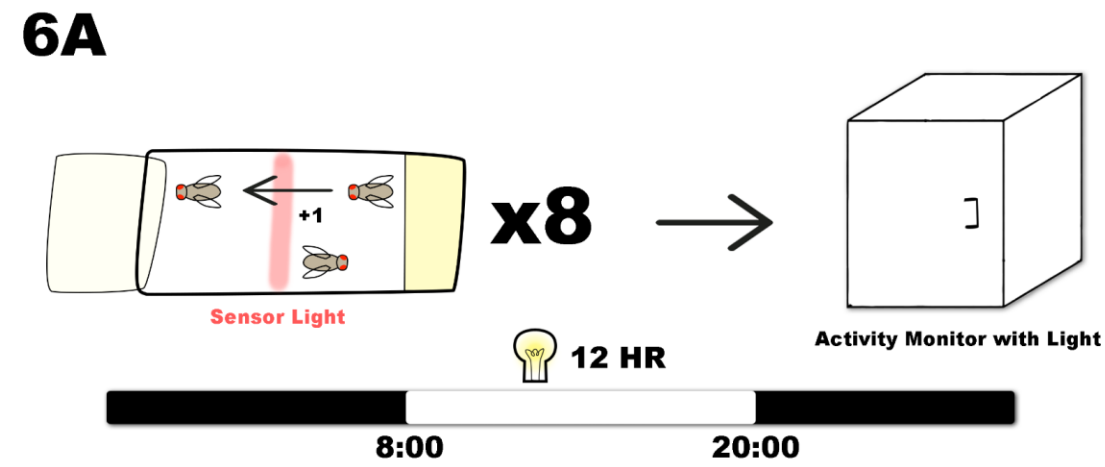

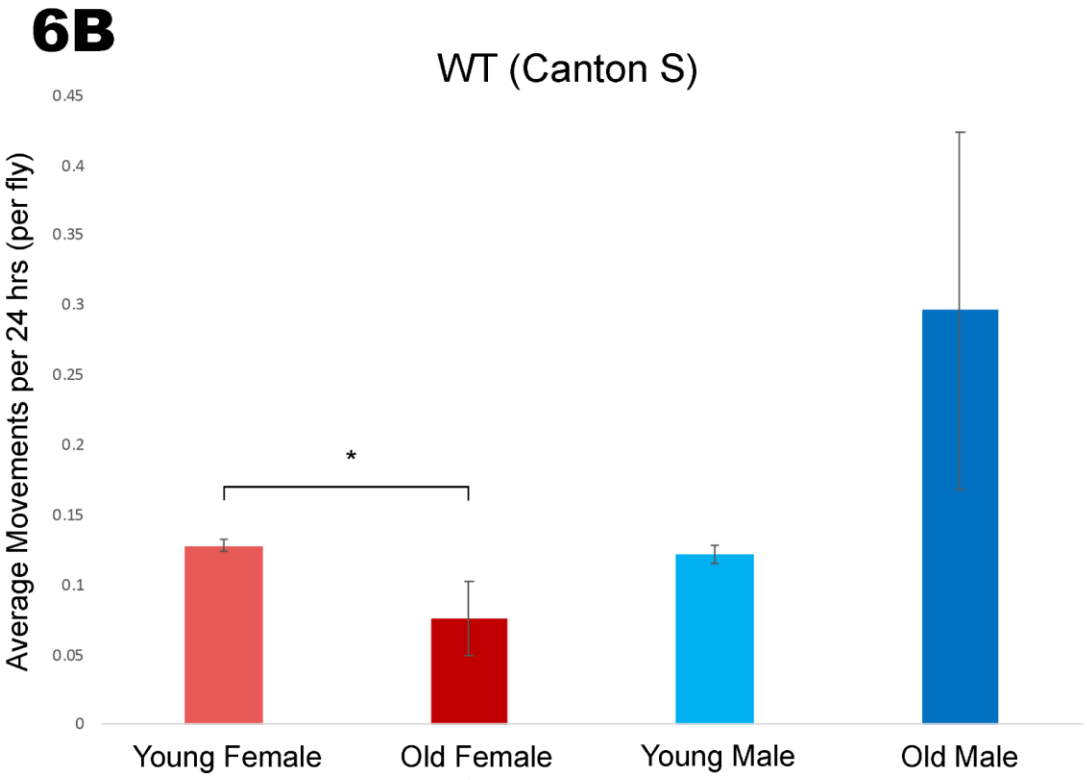

Figure 6: Activity monitor data may robustly show a significant difference between young and old flies in spontaneous activity but more data is needed to confirm in all sexes.

An activity monitor assay using a sensor laser was used to tabulate fly activity over 24 hrs. A. 8 fly tubes containing ~20 flies each were placed into a light-proof activity monitor with a white light inside that goes on at 8:00 and off at 20:00 providing a 12 hr day/night cycle. When a fly moves across the sensor laser in the middle of the tube, one point

is added to the counter. The points are tabulated every 30s. B. 40 young female, 36 old female, 39 young male and 28 old male flies were used. A significant decrease in climbing ability is seen in WT CantonS older female flies as compared to younger female flies (n = 2, ~40 flies per replicate, t(2) = -7.087, p = .029). The results were non-significant between older and younger male flies (n = 2, ~40 flies per replicate, t(2) = 1.344, p = *ns*).

Verification of DAM as Quantification of Circadian Rhythm

The dopaminergic systems disrupted in Parkinson's disease often cause sleep disturbances in humans due to levels of DA functioning as a clock-like molecular mechanism[35,36,40]. The exact changes in circadian rhythm changes tend to vary in humans and it has not been used as a measure of PD in fly models commonly. In this study, we aim to introduce circadian rhythms as a measure of PD in our hTyr flies using 12 hr/12 hr day night cycle activity monitor readings (**Figure 6A**). Additionally, we expect to see age-dependent circadian activity changes in *Drosophila* such that older flies will have flattened circadian curves and experience more erratic sleep periods, similar to our future expectations for hTyr flies[43,44]. Therefore, we aimed to conduct a test using the activity monitor setup using old and young WT CantonS flies to both collect baseline data and establish the model's validity. The data was formatted into 10-minute bins and graphically represented (**Figure 7**). Overall, the young flies exhibited activity similar to what was expected, although more data would be needed to robustly conclude that this would be a satisfactory baseline to work off of, and to see whether the activity shown between 00:00 and 08:00 is significantly higher than expected in young males. Both older fly sexes showed different patterns than their younger counterparts, both showing the flattening of activity throughout the day, though the old male flies behaved more erratically than expected overall.

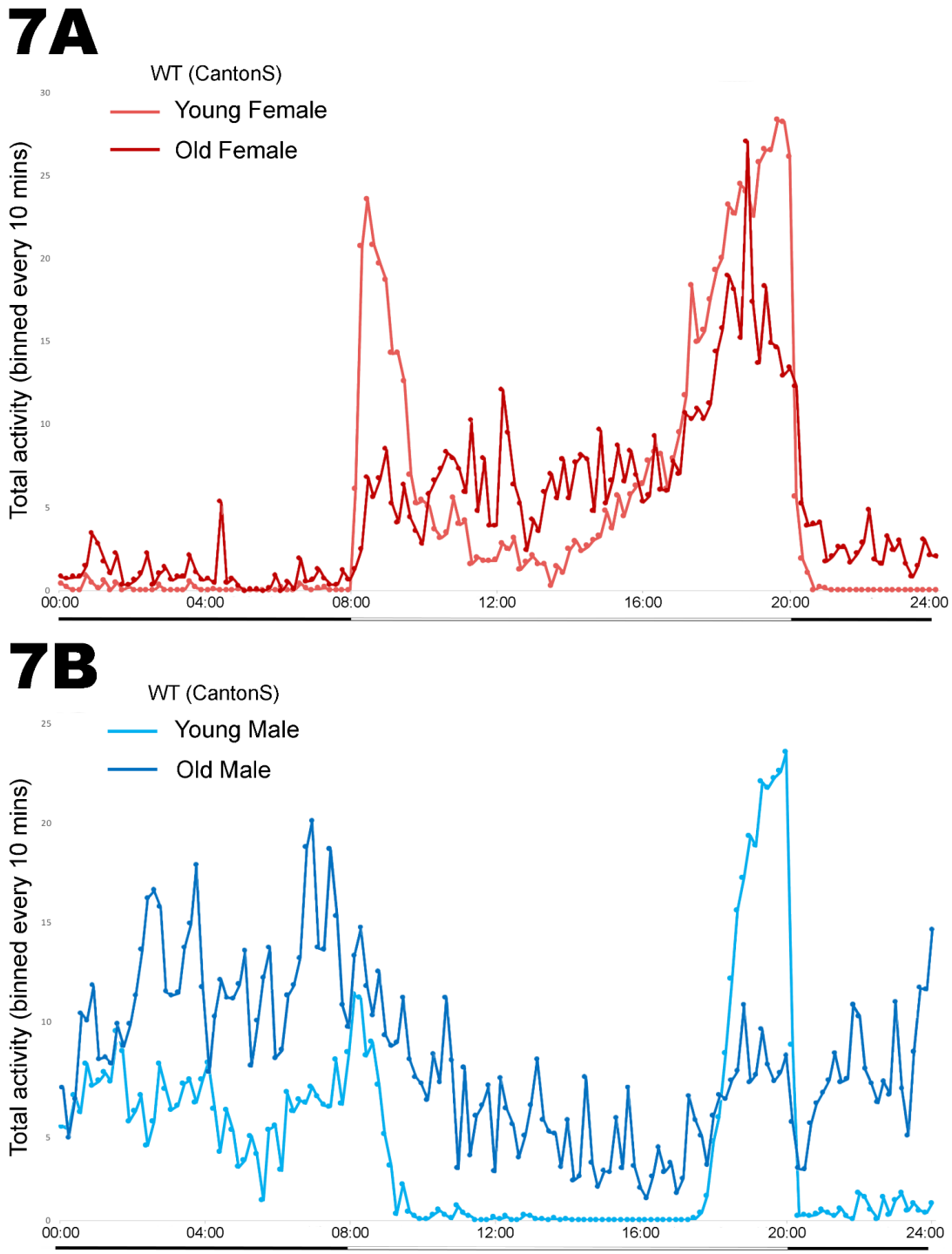

Figure 7: Raw data activity graphs show age-related changes in fly circadian rhythms.

Process for gathering activity data is shown in figure 6A. Data was binned every 10 minutes over a 24-hour period and then graphed. 40 young female, 36 old female, 39 young male and 28 old male flies were used. A. Young female flies show typical circadian patterns such as the spikes of activity at the anticipation of lights-on and lights-off and flattening of activity in-between anticipatory periods and extinction of activity in the lights-off period. Old female flies show decreased activity in the lights-on anticipatory period, increased activity between anticipatory periods, more sporadic activity around the lights-off anticipatory period, and more baseline and sporadic activity in the lights-off period. B. Young male flies show similar patterns to young female flies except for higher activity between 00:00 and 08:00. Old male flies show dramatic increases across the whole day in activity except for muted activity at the lights-off anticipatory period.

To further investigate the trends observed in the raw data (**Figure 7**), we created python code (in supplemental materials) in order to apply Fourier analysis[53] to the activity monitor data and plot periodograms of the results (**Figure 8**). Additionally, Fisher's procedure[54] was used to obtain p-values for each condition. The periodograms show periods (in minutes) with rhythmicity quantified by spectral energy (R^2), with higher spectral energy denoting more robust rhythmicity of activity at that period. In more lay terms, the fourier transform recreates the activity data as a combined series of waveforms and identifies the stronger waveforms (R^2). These are represented in the periodogram by the graphical peaks, and the y-axis of the peak denotes how many minutes are between each crest in the waveform. We can see that for all of the flies, high peaks occur around the 30 and 50 minute period mark (except for young male, which has its second highest peak around 90 minutes), with waning rhythmicity at longer periods. However, it is clear that the rhythmicity is less regular in both older groups, with especially old male showing higher peaks at longer periods, suggesting irregular periodicities that would repeat 3-6 times per day. This suggests a warped circadian rhythm pattern where activity pops up in the night where it is not supposed to.

In addition, both of the old flies show lower R^2 values and lower p values (though the p values for all of the groups were still very small). Lower R^2 values indicate the expected depressing of rhythmicity over fly lifespan, and lower p values indicate reduced confidence in the statistical validity of the rhythmicity.

Fisher's procedure[54] can only determine significance for the maximum R^2, or the highest peak. While other tests of significance do exist for Fourier analysis, their implementation was beyond the scope of this thesis and can be explored in future study. Therefore, in our current approach, this test is most useful to determine the dominant period of the dataset and its relationship to other large periods of the dataset as well as other group datasets. Because our data was limited to a single 24-hour time course, we were only able to identify periodicities under 24 hours in length. We expect based on previous datasets[43,44] for the strongest periodicities to be around 24 hours in all datasets, with less strong and more irregular periodicities in older flies as compared to younger. While this dataset does show reduced strength and higher irregularity in older flies as well as a helpful proof-of-concept for the technique itself, it broadly lacks the ability to draw meaningful conclusions about the day-night cycle in flies at this point. We would recommend that to verify this assay, data be collected over multiple days so that periodicities 24 hours and longer can be adequately explored.

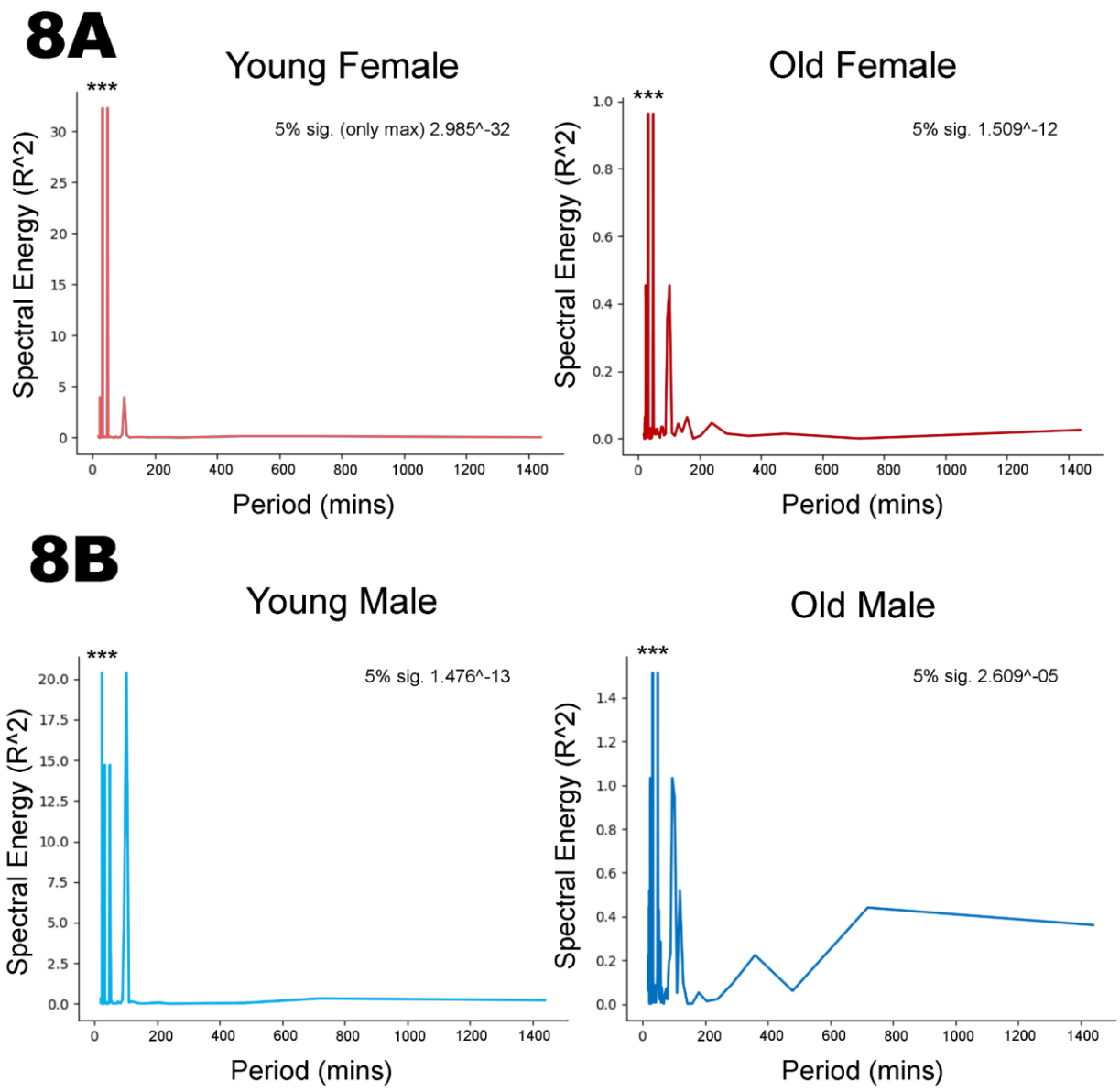

Figure 8: Activity periodograms show significant short activity oscillations and show potential for future use in circadian rhythm analysis with larger datasets.

Using WT CantonS activity monitor data from figure 7 as well as python code (in supplemental), periodograms were plotted. A. Young female flies showed a significant oscillation at 31 mins (Fourier analysis with Fisher's significance analysis, peak R^2 = 32.306 at 31 mins, p = 2.985^{-32}). and old female flies showed a significant oscillation at 35 minutes (Fourier analysis with Fisher's significance analysis, peak R^2 = 0.963 at 35 mins, p = 1.509^{-12}). B. Young male flies showed a significant oscillation at (Fourier analysis with Fisher's significance analysis, peak R^2 = 20.376 at

28 mins, $p = 1.476^{-13}$) and old male flies showed a significant oscillation at 35 minutes (Fourier analysis with Fisher's significance analysis, peak $R^2 = 1.515$ at 35 mins, $p = 2.609^{-05}$).

Discussion

The development of accurate Parkinson's disease models is crucial for the furtherment of Parkinson's disease research–both for understanding its etiology and treatment. Neuromelanin (NM) is a bone-a-fide melanin created in dopaminergic neurons whose function is likely to neutralize harmful oxidative byproducts from the dopaminergic synthesis and breakdown pathway[15,20,21,22]. In the introduction, I review the case that neuromelanin buildup in the lysosomes of dopaminergic neurons is a critical and causal element of PD etiology due to its insolubility contributing to the breakdown of the proteostatic systems in the dopaminergic neurons eventually leading to DA neurodegeneration[15,21,23,25]. Carballo-Carbajal showed that an increase in human tyrosinase (hTyr), which had long been overlooked in favor of tyrosine hydroxylase (TH) in the field[9,17,18], is sufficient for the endogenous production of NM in rat brains and produces rats with highly similar phenotypes and neurological hallmarks to PD (neurodegeneration, inclusions, macroscopically visible SNpc, etc)[15]. Therefore, the goal of this project was to attempt expressing hTyr in *Drosophila* to create a novel Parkinson's disease model that is reflective of a critical piece of human PD etiology and can provide unique advantages for labs looking to study PD.

We began by designing a plasmid to express hTyr in flies, as there currently exists no hTyr *Drosophila* line. We inserted a hTyr-3XFLAG sequence[41] into an existing pUASt-attB *Drosophila*-compatible backbone[45] to make an original UAS-hTyr transgene. We mocked up a combined plasmid in ApE and over the course of the 2022 fall

semester and part of the 2023 spring semester, we cloned the plasmids such that we were able to successfully create the cloned pUASt-attb+hTyr-3XFLAG plasmid (**Figures 1 and 2, supplementary Figure 1**). Flies were transformed with this transgene in March of 2023 and the process of establishing and validating transgenic fly lines is currently underway.

In the gap between shipping our plasmid and receiving back the injected larvae, we decided on driver lines to mate the homozygous hTyr flies with to drive cell type specific transgenic expression of hTyr. As we are using the UAS-GAL4 expression system (**Figure 3A**), we decided on using four lines. First is a WT control, a line that will not express hTyr but would be genetically similar in every other way to the other lines. We will also use ELAV-GAL4/UAS-hTyr, a line that would create flies expressing hTyr in all neurons, and NPF-GAL4/UAS-hTyr, a line that would express hTyr only in NPF-producing neurons (**Figure 3B**). Since hTyr should only successfully produce NM in dopamine-producing neurons, the line containing NPF-GAL4 should not contain any neuromelanin. We will also use ple-GAL4/UAS-hTyr, which should express hTyr in only dopaminergic neurons. ELAV/hTyr will be a comparative control to ple/hTyr, since by our estimates NM should be produced in both lines, but we would be able to observe whether there are any additional effects of hTyr expression in other neurons or if ple failed to express hTyr/NM in some or all dopaminergic neurons. Upon receiving our driver lines we mated them with UAS-GFP flies. This was done such that we could dissect them to verify correct expression patterns and obtain images with which to compare our experimental flies to (as NM granules may be macroscopically viewable[14,19]). We dissected the UAS-GFP flies and imaged them to verify expected

tissue-specific expression and collect images to compare against future dissected UAS-hTyr fly brains (**Figure 4**).

Additionally, we tested our three chosen behavioral assays on wild type (WT) CantonS flies eclosed three weeks apart to test their experimental validity. We tested a staple assay for negative geotaxis in fly PD research, a climbing assay (**Figure 5A**) and found results consistent with our expectations (**Figure 5B**). If we tested hTyr flies of the same age we would expect significantly lower scores on negative geotaxis in all age groups as well as a larger difference between young and old than we saw in CantonS flies.

We used an activity monitor assay (**Figure 6A**) to gain data to use for spontaneous activity analysis (**Figure 6B**) and circadian rhythm analysis (**Figures 7 and 8**). While the female flies behaved as expected in both assays, abnormalities arose with the male flies for both assays, and in both assays we would need more data to verify the robustness of this assay for comparison against the hTyr flies. However, as many of our predictions about the assays' performances were confirmed and most abnormalities could be attributed to low sample sizes, we believe that activity monitor data is useful for quantifying spontaneous activity data and circadian rhythm data and more data should be collected to verify it for use with hTyr flies. If the verification is successful, we would expect hTyr flies to show lower spontaneous activity compared to WT CantonS as well as a higher difference between young and old hTyr flies. We would also expect hTyr flies to show weaker and more irregular periodicity in the circadian rhythm assay than WT CantonS flies as well as a larger difference between young and old hTyr flies as compared to WT CantonS flies.

As of April 2023, the hTyr flies that we received are still being mated to achieve fully homozygous hTyr flies. Those flies will then need to be mated to our chosen driver lines in order to express hTyr. Therefore, this timeline precludes including homozygous hTyr data in this project. Though we cannot test the new line yet, the cloning work in this project is a critical step forward for neuromelanin research and Parkinson's disease research at large, and the work we have completed in verifying the driver lines and assays will be readily used to asses the homozygous hTyr flies in the 2023-2024 year. If we are able to verify successful neuromelanin expression in these flies in the future and verify their phenotypic similarities to other PD fly models, more experiments using these flies could contribute very meaningfully to the field of PD research.

Exploring the tantalizing opportunity first explored in Carballo-Carbajal that lysosomal exocytosis of NM-laden lysosomes can reduce or even reverse PD symptoms in another model organism would be an excellent next step. More research could be done with these flies to determine NM's effect on the mitochondrial degradation system, other PD hallmarks like alpha-synuclein and even genes implicated in PD–potentially illuminating finds for the field. Neuromelanin in Parkinson's disease is a fast-growing field with potential to elucidate the mechanisms behind a mysterious and mounting ailment as well as help find treatments and cures to help real people–hTyr flies can be a real part of that future.

Acknowledgements

I would like to thank Professor Hur, my advisor, first reader and lab leader for graciously providing me a spot in your lab, being a steady hand through the last year,

providing many of the materials for this thesis and overall making this thesis possible. I would like to thank my second reader Professor Duistermars as well for sparking the inspiration for my thesis in his classes and providing constructive feedback throughout the process. I would also like to thank my lab mates Ayame Misaki Bluebell and Param Desagni for aiding with this thesis, especially in the cloning section, and for being willing and eager at all times to jump in and learn. I would like to thank Professor Ruth Halaban and her lab for creating and providing the mammalian hTyr plasmid used in this project. Additionally, I would like to thank my partner Kaia Smith in assisting with the creation of the periodograms featured in figure 8 as well as being incredibly supportive throughout my whole thesis. Lastly, I would like to thank the Keck Science Neuroscience department and Harvey Mudd Biology department for facilitating and supporting the production of this thesis project.

References

1: Medina, L. D., Sabo, S., Vespa, J. (2020). Living Longer: Historical and Projected Life Expectancy in the United States, 1960 to 2060. *Current Population Reports,* U.S. Census Bureau, Washington DC, 25-1145. https://www.census.gov/content/dam/Census/library/publications/2020/demo/p25-1145.pdf

2: Crimmins E. M. (2015). Lifespan and Healthspan: Past, Present, and Promise. *The Gerontologist*, *55*(6), 901–911. https://doi.org/10.1093/geront/gnv130

3: Rappuoli, R. (2014). Vaccines: Science, health, longevity, and wealth. *PNAS, 111*(34), 12282. https://doi.org/10.1073/pnas.1413559111

4: Niccoli, T., Partridge, L. (2012). Ageing as a Risk Factor for Disease. *Current Biology, 22*(17), R741-R752. https://doi.org/10.1016/j.cub.2012.07.024

5: Jellinger K. A. (2010). Basic mechanisms of neurodegeneration: a critical update. *Journal of cellular and molecular medicine*, *14*(3), 457–487. https://doi.org/10.1111/j.1582-4934.2010.01010.x

6: Zeng, X. S., Geng, W. S., Jia, J. J., Chen, L., & Zhang, P. P. (2018). Cellular and Molecular Basis of Neurodegeneration in Parkinson Disease. *Frontiers in aging neuroscience*, *10*, 109. https://doi.org/10.3389/fnagi.2018.00109

7: World Health Organization. (2022). Parkinson Disease. https://www.who.int/news-room/fact-sheets/detail/parkinson-disease

8: National Institute on Aging. (2022). Parkinson's Disease: Causes, Symptoms, and Treatments. https://www.nia.nih.gov/health/parkinsons-disease

9: Fahn S. (2015). The medical treatment of Parkinson disease from James Parkinson to George Cotzias. *Movement disorders : official journal of the Movement Disorder Society*, *30*(1), 4–18. https://doi.org/10.1002/mds.26102

10: Lees, A. J., Tolosa, E., & Olanow, C. W. (2015). Four pioneers of L-dopa treatment: Arvid Carlsson, Oleh Hornykiewicz, George Cotzias, and Melvin Yahr. *Movement disorders : official journal of the Movement Disorder Society*, *30*(1), 19–36. https://doi.org/10.1002/mds.26120

11: Carlsson A. The occurrence, distribution and physiological role of catecholamines in the nervous system. *Pharmacol Rev* 1959:11:490–493.

12: Carlsson A. A half-century of neurotransmitter research: impact on neurology and psychiatry. Nobel Lecture, December 8, 2000. In: http://www.nobelprize.org/nobel_prizes/medicine/laureates/2000/carlsson-lecture.pdf

13: Cotzias GC, Van Woert MH, Schiffer LM. Aromatic amino acids and modification of parkinsonism. *N Engl J Med* 1967;276:374–379.

14: Lees, A. J., Selikhova, M., Andrade, L. A., & Duyckaerts, C. (2008). The black stuff and Konstantin Nikolaevich Tretiakoff. *Movement disorders : official journal of the Movement Disorder Society*, *23*(6), 777–783. https://doi.org/10.1002/mds.21855

15: Carballo-Carbajal, I., Laguna, A., Romero-Giménez, J., Cuadros, T., Bové, J., Martinez-Vicente, M., Parent, A., Gonzalez-Sepulveda, M., Peñuelas, N., Torra, A., Rodríguez-Galván, B., Ballabio, A., Hasegawa, T., Bortolozzi, A., Gelpi, E., & Vila, M. (2019). Brain tyrosinase overexpression implicates age-dependent neuromelanin production in Parkinson's disease pathogenesis. *Nature communications*, *10*(1), 973. https://doi.org/10.1038/s41467-019-08858-y

16: Nagatsu T, Levitt M, Udenfriend S. Tyrosine hydroxylase: the initial step in norepinephrine biosynthesis. *J Biol Chem* 1964;239:2910–1917.

17: Tabrez, S., Jabir, N. R., Shakil, S., Greig, N. H., Alam, Q., Abuzenadah, A. M., Damanhouri, G. A., & Kamal, M. A. (2012). A synopsis on the role of tyrosine hydroxylase in Parkinson's disease. *CNS & neurological disorders drug targets*, *11*(4), 395–409. https://doi.org/10.2174/187152712800792785

18: Nagatsu, T., Nakashima, A., Watanabe, H., Ito, S., & Wakamatsu, K. (2022). Neuromelanin in Parkinson's Disease: Tyrosine Hydroxylase and Tyrosinase.

International journal of molecular sciences, *23*(8), 4176. https://doi.org/10.3390/ijms23084176

19: MARSDEN C. D. (1961). Pigmentation in the nucleus substantiae nigrae of mammals. *Journal of anatomy*, *95*(Pt 2), 256–261.

20: Bush, W. D., Garguilo, J., Zucca, F. A., Albertini, A., Zecca, L., Edwards, G. S., Nemanich, R. J., & Simon, J. D. (2006). The surface oxidation potential of human neuromelanin reveals a spherical architecture with a pheomelanin core and a eumelanin surface. *Proceedings of the National Academy of Sciences of the United States of America*, *103*(40), 14785–14789. https://doi.org/10.1073/pnas.0604010103

21: Vila, M. (2019). Neuromelanin, aging, and neuronal vulnerability in Parkinson's disease. *Movement disorders : official journal of the Movement Disorder Society*, *34*(10), 1440–1451. https://doi.org/10.1002/mds.27776

22: Zucca, F. A., Basso, E., Cupaioli, F. A., Ferrari, E., Sulzer, D., Casella, L., & Zecca, L. (2014). Neuromelanin of the human substantia nigra: an update. *Neurotoxicity research*, *25*(1), 13–23. https://doi.org/10.1007/s12640-013-9435-y

23: Sulzer, D., Mosharov, E., Talloczy, Z., Zucca, F. A., Simon, J. D., & Zecca, L. (2008). Neuronal pigmented autophagic vacuoles: lipofuscin, neuromelanin, and ceroid as macroautophagic responses during aging and disease. *Journal of neurochemistry*, *106*(1), 24–36. https://doi.org/10.1111/j.1471-4159.2008.05385.x

24: Halliday, G. M., Fedorow, H., Rickert, C. H., Gerlach, M., Riederer, P., & Double, K. L. (2006). Evidence for specific phases in the development of human neuromelanin. *Journal of neural transmission (Vienna, Austria : 1996)*, *113*(6), 721–728. https://doi.org/10.1007/s00702-006-0449-y

25: Hara, T., Nakamura, K., Matsui, M., Yamamoto, A., Nakahara, Y., Suzuki-Migishima, R., Yokoyama, M., Mishima, K., Saito, I., Okano, H., & Mizushima, N. (2006). Suppression of basal autophagy in neural cells causes neurodegenerative disease in mice. *Nature*, *441*(7095), 885–889. https://doi.org/10.1038/nature04724

26: https://www.ncbi.nlm.nih.gov/pmc/articles/PMC4496713/

27: Wakamatsu K., Murase T., Zucca F.A., Zecca L., Ito S. Biosynthetic pathway to neuromelanin and its aging process. *Pigment Cell Melanoma Res.* 2012;25:792–803. doi: 10.1111/pcmr.12014.

28: Greggio, E. et al. Tyrosinase exacerbates dopamine toxicity but is not genetically associated with Parkinson's disease. *J. Neurochem.* 93, 246–256 (2005).

29: Xu, Y. et al. Tyrosinase mRNA is expressed in human substantia nigra. *Brain Res. Mol. Brain Res.* 45, 159–162 (1997).

30: Sanchez-Ferrer, A., Rodriguez-Lopez, J. N., Garcia-Canovas, F. & Garcia-Carmona, F. Tyrosinase: a comprehensive review of its mechanism. *Biochim. Biophys. Acta* 1247, 1–11 (1995).

31: Jennings, B. H. (2011). *Drosophila* - a versatile model in biology & medicine. *Materials Today*, *14*(5), 190–195. https://doi.org/10.1016/S1369-7021(11)70113-4

32: Chiang, A-S., et al. (2011). Three-Dimensional Reconstruction of Brain-wide Wiring Networks in *Drosophila* at Single-Cell Resolution. *Current Biology*, *21*(1), 1–11. https://doi.org/10.1016/j.cub.2010.11.056

33: Feany, M., Bender, W. (2000) A *Drosophila* model of Parkinson's disease. *Nature,* 404, 394–398. https://doi.org/10.1038/35006074

34: Aggarwal, A., Reichert, H., & VijayRaghavan, K. (2019). A locomotor assay reveals deficits in heterozygous Parkinson's disease model and proprioceptive mutants in adult *Drosophila*. *Proceedings of the National Academy of Sciences of the United States of America*, *116*(49), 24830–24839.

35: Willison, L. D., Kudo, T., Loh, D. H., Kuljis, D., & Colwell, C. S. (2013). Circadian dysfunction may be a key component of the non-motor symptoms of Parkinson's disease: insights from a transgenic mouse model. *Experimental neurology*, *243*, 57–66. https://doi.org/10.1016/j.expneurol.2013.01.014

36: Stefani, A., & Högl, B. (2020). Sleep in Parkinson's disease. *Neuropsychopharmacology : official publication of the American College of Neuropsychopharmacology*, *45*(1), 121–128. https://doi.org/10.1038/s41386-019-0448-y

37: Refinetti, R., Lissen, G. C., & Halberg, F. (2007). Procedures for numerical analysis of circadian rhythms. *Biological rhythm research*, *38*(4), 275–325. https://doi.org/10.1080/09291010600903692

38: Brand, A. H., and N. Perrimon. “Targeted Gene Expression as a Means of Altering Cell Fates and Generating Dominant Phenotypes.” *Development (Cambridge, England)*, vol. 118, no. 2, June 1993, pp. 401–15.

39: Chung, B. Y., Ro, J., Hutter, S. A., Miller, K. M., Guduguntla, L. S., Kondo, S., & Pletcher, S. D. (2017). Drosophila Neuropeptide F Signaling Independently Regulates Feeding and Sleep-Wake Behavior. *Cell reports*, *19*(12), 2441–2450. https://doi.org/10.1016/j.celrep.2017.05.085

40: Logan, R. W., Parekh, P. K., Kaplan, G. N., Becker-Krail, D. D., Williams, W. P., 3rd, Yamaguchi, S., Yoshino, J., Shelton, M. A., Zhu, X., Zhang, H., Waplinger, S.,

Fitzgerald, E., Oliver-Smith, J., Sundarvelu, P., Enwright, J. F., 3rd, Huang, Y. H., & McClung, C. A. (2019). NAD+ cellular redox and SIRT1 regulate the diurnal rhythms of tyrosine hydroxylase and conditioned cocaine reward. *Molecular psychiatry*, *24*(11), 1668–1684. https://doi.org/10.1038/s41380-018-0061-1

41: Halaban, R., Cheng, E., & Hebert, D. N. (2002). Coexpression of wild-type tyrosinase enhances maturation of temperature-sensitive tyrosinase mutants. *The Journal of investigative dermatology*, *119*(2), 481–488. https://doi.org/10.1046/j.1523-1747.2002.01824.x

42: Shaltiel-Karyo, R., et al. (2020). A Novel, Sensitive Assay for Behavioral Defects in Parkinson's Disease Model *Drosophila*. *Hindawi*, Article ID 697564. https://doi.org/10.1155/2012/697564

43: Koh, K., Evans, J. M., Hendricks, J. C., & Seghal A. (2006). A *Drosophila* model for age-associated changes in sleep:wake cycles. *PNAS, 103*(37), 13843-13847. https://doi.org/10.1073/pnas.0605903103

44: De Nobrega, A. K., & Lyons, L. C. (2020). Aging and the clock: Perspective from flies to humans. *The European journal of neuroscience*, *51*(1), 454–481. https://doi.org/10.1111/ejn.14176

45: Groth, A. C., Fish, M., Nusse, R., Calos, M. P. (2003). Construction of Transgenic Drosophila by Using the Site-Specific Integrase From Phage φC31. *Genetics, 166*(4), 1775-1782. doi: 10.1534/genetics.166.4.1775

46: Mousavi, S. M., Zarei, M., Hashemi, S. A. (2018). Polydopamine for Biomedical Application and Drug Delivery System. *Medicinal Chemistry (Los Angeles), 8*(8), 218-229. doi: 10.4172/2161-0444.1000516

47: Haining, R. L., & Achat-Mendes, C. (2017). Neuromelanin, one of the most overlooked molecules in modern medicine, is not a spectator. *Neural regeneration research*, *12*(3), 372–375. https://doi.org/10.4103/1673-5374.202928

48: Sulzer, D., Cassidy, C., Horga, G., Kang, U. J., Fahn, S., Casella, L., Pezzoli, G., Langley, J., Hu, X. P., Zucca, F. A., Isaias, I. U., & Zecca, L. (2018). Neuromelanin detection by magnetic resonance imaging (MRI) and its promise as a biomarker for Parkinson's disease. *NPJ Parkinson's disease*, *4*, 11. https://doi.org/10.1038/s41531-018-0047-3

49: Dumitrescu, E., Copeland, J. M., & Venton, B. J. (2023). *Parkin* Knockdown Modulates Dopamine Release in the Central Complex, but Not the Mushroom Body Heel, of Aging *Drosophila*. *ACS chemical neuroscience*, *14*(2), 198–208. https://doi.org/10.1021/acschemneuro.2c00277

50: Pu, Y., Zhang, Y., Zhang, Y., & Shen, P. (2018). Two Drosophila Neuropeptide Y-like Neurons Define a Reward Module for Transforming Appetitive Odor Representations to Motivation. *Scientific reports*, *8*(1), 11658. https://doi.org/10.1038/s41598-018-30113-5

51: Davis, M. W. & Jorgensen, E. M. (2022) ApE, A Plasmid Editor: A Freely Available DNA Manipulation and Visualization Program. *Front. Bioinform. 2*(818), 619. doi: 10.3389/fbinf.2022.818619

52: Schneider, C.A., Rasband, W.S., Eliceiri, K.W. (2012) NIH Image to ImageJ: 25 years of image analysis. *Nature Methods, 9*, 671-675.

53: Refinetti, R., Lissen, G. C., & Halberg, F. (2007). Procedures for numerical analysis of circadian rhythms. *Biological rhythm research*, *38*(4), 275–325. https://doi.org/10.1080/09291010600903692

54: Fisher, R. A. (1929). Tests of significance in harmonic analysis. *Proceedings of the Royal Society of London. Series A, Containing Papers of a Mathematical and Physical Character*, *125*(796), 54-59. Google Scholar

55: Calos M. P. (2006). The phiC31 integrase system for gene therapy. *Current gene therapy*, *6*(6), 633–645. https://doi.org/10.2174/156652306779010642

Supplementary Information

Cloning primers

Primers used to isolate the hTyr CDS via PCR:

Forward primer, hTYR_SfiI_F: CGCAG GGCCGGACGGGCC CTG CTC CTG GCT GTT TTG TA

Reverse primer, hTYR_SfiI_R: CGCAG GGCCCCAGTGGCC GGA TGC CAC CCG GGA TCA

Primers used to validate and sequence clones via PCR:

5’ end, forward primer (inside hsp70 promoter): ATCAATTAAAAGTAACCAGCAACCAA

5’ end, reverse primer (inside hTYR), hTYR_cloning_V_R: CTC GGG CGT TCC ATT GCA TA

If cloning works, amplicon would be 1005 bases long.

3’ end, forward primer (inside hTYR), hTYR_cloning_V_F: CCA GCA TCA TTC TTC TCC TC

3’ end, reverse primer (inside SV40 terminator):

GTATAATGTGTTAAACTACTGATTCTAAT

If cloning works, amplicon would be 1092 bases long.

Restriction Fragment Mapping

Plating, inoculation and a midi prep were performed to isolate the plasmid DNA from bacteria. Gel electrophoresis was performed to verify the success of these procedures. Once the DNA was isolated properly, a restriction digest with three restriction enzymes and subsequent verification gel electrophoresis were performed in order to verify the identity of the hTyr DNA (**supplementary Figure 1A**). After successful verification, the hTyr+3xFLAG was amplified with PCR.

We then performed purification on the first PCR sample we had, digested it using SfiI, transformed it into cells and plated those cells to attempt to get bacterial colonies with the cloned plasmids. A gel was used to verify the success of the purification procedure. Nanodrop confirmed that colonies 1 and 5 contained a sufficient amount of DNA to proceed to identification with, and a BAMH1 digest and sequencing using our designed verification primers revealed that both colonies contained the cloned plasmid (**supplementary Figure 1B**). The clones were additionally sequenced to verify successful ligation. The cloned plasmid was successfully injected into fly larvae (Rainbow Transgenic Flies Incorporated, Camarillo CA). The overall process is simplified in figure 2.

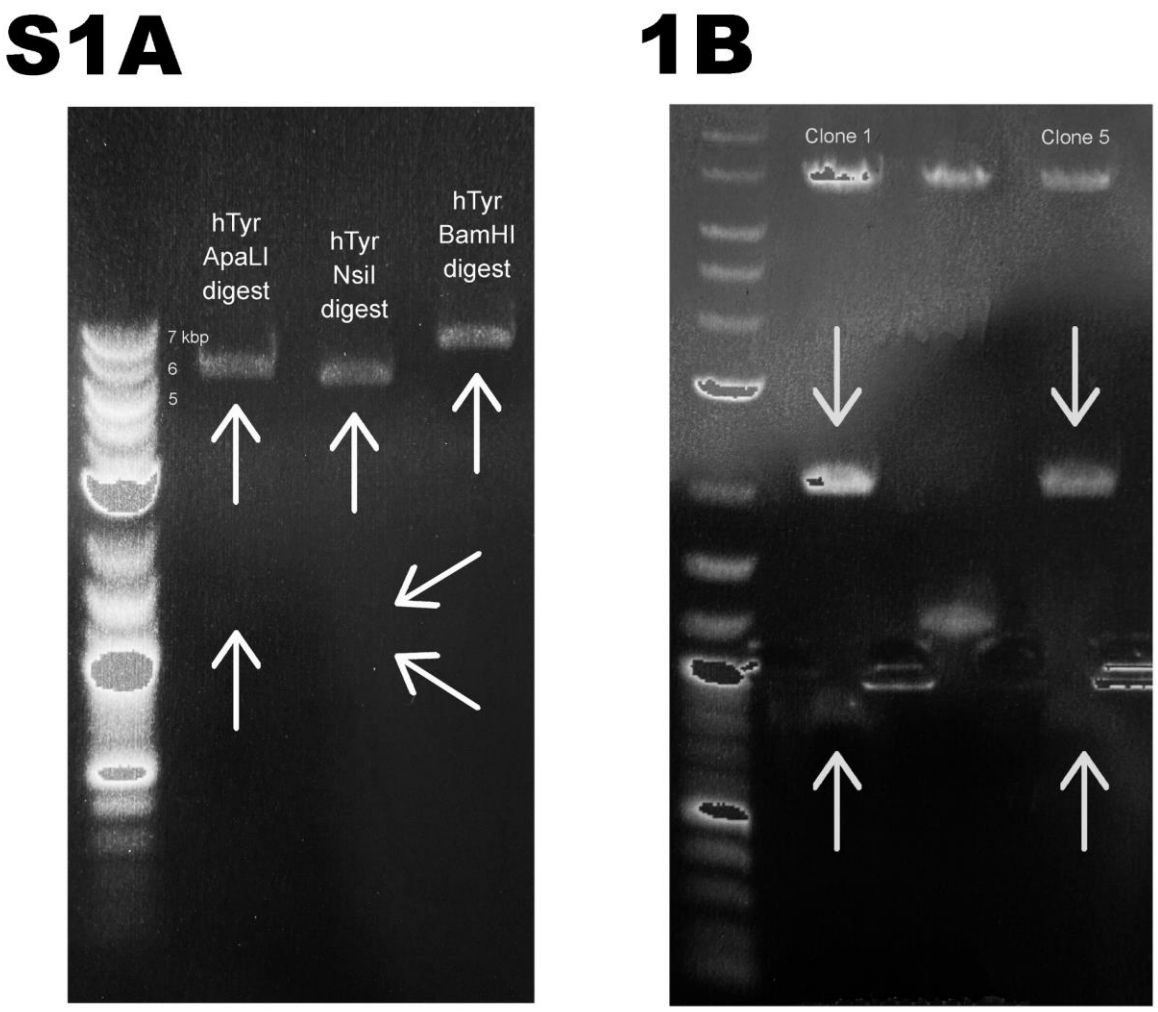

Supplementary Figure 1: Gels for the validation of hTyr plasmid identity and cloned plasmid identity.

A. This gel contains three restriction digests of the hTyr plasmid using three different enzymes. The ApaLI digest was expected to produce two bands at 6.6kb and 1.2kb, both of which are in the gel. The NsiI digest was expected to produce five fragments at 5.8kb, 0.9kb, 0.6kb, 0.4kb and 0.07kb. The 5.8kb band can be clearly seen, while the 0.9 and 0.6kb bands can be faintly seen. The BamHI was expected to produce two fragments, 7.8kb and 0.1kb. The 7.8kb band is clearly shown, while the 0.1kb band is obscured by runoff. B. This gel contains the DNA from three bacterial colonies thought to contain the cloned pUASt+hTyr plasmid. BamHI digest was done to validate the presence of the DNA in the cloned colonies. The expected 2kb and 1kb diagnostic bands can be clearly seen in clones 1 and 5. The middle band contains a different clone, the 1.2kb band is a residue of the un-ligated pUASt plasmid.

Fourier Analysis Code

```
import math
import matplotlib.pyplot as plt
import pandas as pd
#use terminal to determine path to reach desired excel file
data  = pd.read_excel(r'/Users/loricallan/Desktop/Fall Semester 2022 + Spring
Semester 2023/Thesis/Data +  Analysis/CircadianPythonData.xlsx')

#df = pd.DataFrame(data, columns = ['1', '2', '3', '4']), make sure to name first row
1,2,3,4, etc. above data, each variable can only be a single column
YoungFemale = data[1].values.tolist()
YoungMale = data[2].values.tolist()
OldFemale = data[3].values.tolist()
OldMale  = data[4].values.tolist()
#define each of your data columns as a newly named string

a = []
b = []

N = len(YoungFemale)

def _find_aj(j, x, t):
    val = 0
    N = len(x)
    for i in range(N):
        val += x[i]*math.cos(2*math.pi*j*t[i]/N)
    return 2*val/N

def _find_bj(j, x, t):
    val = 0
    N = len(x)
    for i in range(N):
        val += x[i]*math.sin(2*math.pi*j*t[i]/N)
    return 2*val/N

def calc_vectors(x):
    R_squared = []
    N = len(x)
    t = [10*i for i in range(N)]
    jvec  = list(range(int((N - 1)/2)))[1:]
    for j in jvec:
        val = _find_aj(j, x, t)**2 + _find_bj(j, x, t)**2
        #above is the R^2 value formula
        R_squared.append(val)

    frequency = [j/N for j in jvec]
```

```
    period = [1/f for f in frequency]
    return R_squared, period

R_squared, period = calc_vectors(OldMale)
#switch out 'OldMale'in parenthesis to desired group
g = max(R_squared)/sum(R_squared)
significance = N*(1 - g)**(N - 1)
sig_vec = [significance for x in period]

#print('hi')
#print(R_squared)
#print(period)
plt.clf() # clears the Figure
plt.plot(period, R_squared, label = 'R^2')
#plt.plot(period, sig_vec, label = 'significance')
plt.legend()
plt.show()
```